Thin Solid Films 543 (2013) 51–55

Contents lists available at ScienceDirect

Thin Solid Films

journal homepage: www.elsevier.com/locate/tsf

Transient reflectivity on vertically aligned single-wall carbon nanotubes

Gianluca Galimberti [a], Stefano Ponzoni [a], Gabriele Ferrini [a], Stephan Hofmann [b], Muhammad Arshad [c,d,e], Cinzia Cepek [f], Stefania Pagliara [a,*]

[a] Interdisciplinary Laboratory for Advanced Materials Physics (i-LAMP) and Dipartimento di Matematica e Fisica, Università Cattolica del Sacro Cuore, I-25121 Brescia, Italy
[b] Department of Engineering, University of Cambridge, Cambridge CB3 0FA, UK
[c] Zernike Institute for Advanced Materials, University of Groningen, The Netherlands
[d] ICTP, Strada Costiera 11, I-34151 Trieste, Italy
[e] National Centre for Physics Quaid-i-Azam University Islamabad, Pakistan
[f] Istituto Officina dei Materiali — CNR, Laboratorio TASC, Area Science Park, Basovizza, I-34149 Trieste, Italy

ARTICLE INFO

Available online 13 March 2013

Keywords:
Single-wall carbon nanotubes
Time resolved optical spectroscopy
Excitons

ABSTRACT

One-color transient reflectivity measurements are carried out on two different samples of vertically aligned single-wall carbon nanotube bundles and compared with the response recently published on unaligned bundles. The negative sign of the optical response for both samples indicates that the free electron character revealed on unaligned bundles is only due to the intertube interactions favored by the tube bending. Neither the presence of bundles nor the existence of structural defects in aligned bundles is able to induce a free-electron like behavior of the photoexcited carriers. This result is also confirmed by the presence of non-linear excitonic effects in the transient response of the aligned bundles.

1. Introduction

In these last twenty years carbon nanotubes (CNT) have played a fundamental role in the research field of nanotechnology based optoelectronics and in particular for application in solar cells and sensor devices. The outstanding and intriguing physical properties of CNT including well defined optical resonances, ultrafast non-linear response and ballistic 1D charge transport, have, in fact, stimulated both fundamental and applied research on these systems [1,2].

For increasing the CNT potentialities in optoelectronics, a growing effort, in these last years, has been focused in preparing single-wall CNT (SWCNT) samples with a well-defined chirality [3,4]. The low energy optical properties, in fact, of SWCNT are associated with the formation of electron-hole pairs described as 1D Wannier–Mott excitons. The physical properties of these excitons strongly depend on the tube diameter and chirality [5,6].

The possibility of studying the optical response of SWCNT thin film for different architectures (unaligned, horizontally and vertically aligned tubes; isolated or bundled tubes) with a well defined electronic structure represents at the moment a challenge. Thin films of CNT, deposited, under controlled atmosphere, by using standard techniques such as chemical vapor deposition (CVD) or high pressure carbon monoxide (HiPCo), contain a broad distribution of aggregated tubes with different diameters and chiralities. The optical devices based on CNT thin film, showing the best performance, usually contain semiconducting and metallic tubes with different structures, combined with several other systems (nano-particles, molecules, metallic connector, substrate…) [2,7]. Therefore, in order to improve the performance of the CNT based optical devices, a deeper understanding of the optical properties of thin films containing different tubes is necessary.

In particular, a study of charge carriers dynamics, charge transfer and charge transport into and among the different parts of the whole system is necessary for increasing the efficiency of the carbon based devices, choosing the better configuration and the most useful components. Recently, we have shown that the architecture of CNT thin films strongly affects the charge carrier dynamics [8]. In particular, by using transient reflectivity measurements, we have demonstrated that the combination of bundling and unalignment in carbon nanotube induces strong intertube interactions favoring the formation of short-living free charge carriers in semiconducting tubes. Some of these charge carriers decay through a charge transfer nonradiative process toward the metallic tubes within 400 fs.

Here, by using the same experimental technique, we show that the bundling alone without the unalignment as well as the presence of defects is not enough to generate this kind of free charge carriers. Performing one-color transient reflectivity measurements, in a pump probe experimental set up, on vertically aligned SWCNT, we reveal a response of the photoinduced charge carriers comparable with the exciton-like behavior observed in literature on isolated SWCNT. Photobleaching channels and non-linear effects, only measurable when the probability of creating two or more excitons per nanotube is non-negligible [9,10], are clearly revealed in the transient optical response.

* Corresponding author. Tel.: +39 030 2406 711; fax: +39 030 2406 742.
E-mail address: pagliara@dmf.unicatt.it (S. Pagliara).

0040-6090/$ – see front matter © 2013 Elsevier B.V. All rights reserved.
http://dx.doi.org/10.1016/j.tsf.2013.02.133

2. Experimental details

Vertically aligned CNT bundles (Sample A and Sample B) were synthesized in two different laboratories. Sample A was synthesized in the Department of Engineering at the Cambridge University. The CVD process was done on sputter deposited 10 nm of Al_2O_3 on Si/SiO_2(200 nm). Fe catalyst (1.1 nm) was thermally evaporated onto Al_2O_3. Atmospheric pressure CVD was conducted in a tube furnace at 750 °C in a mixture of $C_2H_2/H_2/Ar$ (30 min) after a 3 min pre-treatment in H_2/Ar. Sample B was grown in the Analytical Division of the TASC-IOM-CNR Laboratory, where the catalyst depositions and CVD processes are performed in an ultra high vacuum experimental apparatus (base pressure $<1 \times 10^{-8}$ Pa). The CVD processes were done on thin films of 150 nm thermally grown SiO_2 support layer on polished n-type Si(100) substrates and on 10 nm thick Al_2O_3 support layers grown via magnetron sputtering on the previous film. We used Fe as catalyst, and acetylene as the precursor gas. Fe catalyst films were deposited in-situ by sublimation from heated filaments (Aldrich, 99.9% purity) at a growth rate of ~0.6 nm/h. We operate in the following parameter window: ~0.6–8 nm Fe film thickness, 4×10^{-6}–10^{-1} Pa C_2H_2 pressure and 580–600 °C growth temperature.

Both samples were characterized by micro-Raman and SEM (Scanning Electron Microscope) measurements. Micro-Raman measurements on Sample A were carried out using a Labram Dilor Raman H10 spectrometer equipped with an Olympus microscope and with a cooled CCD camera as photodetector. The 632.8 nm light from an He–Ne laser was used as the excitation radiation. Micro-Raman measurements on Sample B were carried out using Renishaw 1000 Raman Spectrometer (Series 1000). The spectra were excited with an Ar^+ laser (514.5 nm). SEM images were acquired on both samples ex-situ, after the growth, by using a ZEISS SEM (mod. Supra 40, energy range 0.1–30 KeV).

Time-resolved reflectivity (TR) measurements have been performed with a cavity-dumped Ti:Sapphire oscillator, producing 120 fs, 1.55 eV light pulses. The samples have been excited with pump fluences ranging from 0.1 to 0.8 mJ/cm^2.

3. Results and discussion

In Fig. 1, TR signals collected on two vertically aligned SWCNT bundles (Sample A (a), Sample B (b)) are shown together with SEM images. While the TR signal on unaligned SWCNT is positive (see Fig. 2 of Ref. [8]) in agreement with the free-electron behavior of the photoinduced carriers, TR signal on aligned SWCNT is negative.

The negative signal has been interpreted as a photobleaching process [11,12]. When the pump photon energy is quasi-resonant with one of the optical transition between two Van Hove Singularities (VHSs), a photobleaching is usually expected in the one-color transient optical measurements. Absorption of the pump pulse excites electrons into the conduction band, creating holes in the valence band. Until these carriers relax, transient filling effects on the final states are observed. For the photobleaching effect, the transient signal is positive in trasmittivity and negative in reflectivity (such as in the absorption) [13,14]. The presence of the photobleaching channel in aligned SWCNT bundles suggests that the free-electron like behavior of the photoinduced carriers [8] is due to the unalignment of the bundles and not to the formation of bundles themselves.

In order to exclude that the presence of structural defects affects the charge carrier dynamics of SWCNT, in Fig. 1 the transient reflectivity response has been shown for two SWCNT bundles with a different content of structural defects. In Fig. 2 Raman spectra collected on Sample A and Sample B by using an excitation wavelength of 632.8 nm (for Sample A) and 514.5 nm (for sample B) are reported. The D and the G modes are at about 1300 and 1700 cm^{-1}, the G′ mode at 2600 cm^{-1} and the radial breathing modes (RBM) modes in the (150 cm^{-1}, 250 cm^{-1}) range [15]. Raman spectrum of Sample B is characterized by an intense D mode [16], because the ratio I(D)/I(G) increases with the excitation wavelength, the D mode suggests the significant presence of structural defects in this sample.

It is important to underline that in Sample B the large presence of defects is in anyway compatible with a predominant content of sp^2 hybridization of C atoms in the nanotube walls. The energy position of the G mode (about 1590 cm^{-1}) and the ratio I(D)/I(G) = 0.9, in agreement with the graph taken from ref. [17,18], argue that nanotubes are mainly composed of sp^2-hybridized C atoms even if the significant presence of defects clearly indicates that the wall is composed of clusters and not of homogeneous graphene sheet.

From the analysis of the RBM mode, it is possible to estimate the average diameter of the carbon nanotubes and then by using the Kataura scheme [19] to evaluate the energy positions of the VHSs in both samples. In Sample B the RBM are principally located around

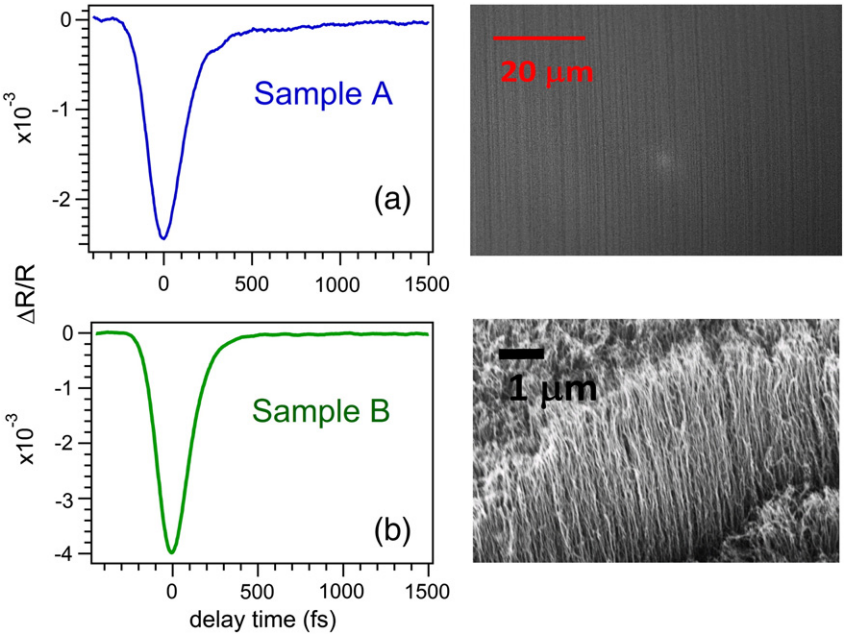

Fig. 1. One-color ($h\nu = 1.55$ eV) transient reflectivity spectra collected on vertically aligned (Sample A (a) and Sample B (b)). The SEM images of the samples are also reported.

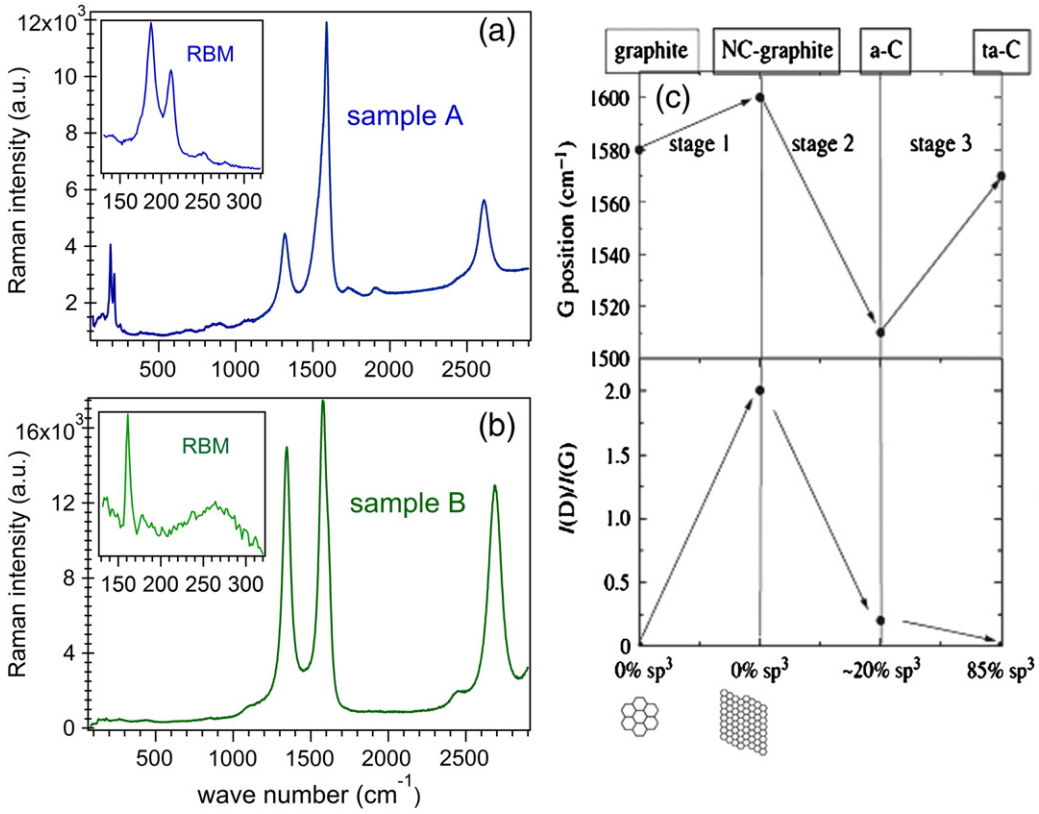

Fig. 2. Raman spectra collected on Sample A (a) and Sample B (b) by using a laser wavelength of 632.8 nm and 514.5 nm, respectively. The intensity of the D mode in the Sample B suggests a significant presence of structural defects in this sample. (c) Graph adapted from ref. [17] to estimate the content of sp^2, sp^3 hybridization in Sample A and B.

160 cm^{-1} (sharp structure) and 270 cm^{-1} (broad structure) corresponding to a diameter ranging from 0.9 nm to 1.55 nm. In the Kataura scheme [19] these diameters indicate that the second VHS (E_{22}) is located at about 1.15 eV and 1.7 eV, respectively. On the contrary, in Sample A, the RBM are located around 185 cm^{-1} and 215 cm^{-1} corresponding to a diameter of 1.4 nm and 1.2 nm. From the Kataura plot, the second VHS results at about 1.2 eV–1.45 eV. For both samples, the pump photon energy (1.5 eV) is able to populate the second VHS giving rise to a photobleaching channel in the transient reflectivity (Fig. 1).

However, by interpolating the transient response, a difference in the reflectivity of the two aligned bundles appears. While Sample A is well fitted by two exponential decays, Sample B is interpolated only by one exponential curve (Fig. 3a and b). In both samples, the resulting decay time of the first dynamics (90 ± 10 fs for Sample A (c) and 65 ± 15 fs for Sample B (d)) is compatible with the relaxation time from the second excitonic level E_{22} to the first one E_{11} [20,21,13]. The linear trend of the first decay time against the pump fluence (Fig. 3c, d) leads to exclude radiative processes [22]. Concerning the second dynamics (with a relaxation time of about 1 ps) of Sample A transient signal, it is usually ascribed in SWCNT to non-linear excitonic effects [9].

A picture of the dynamics in this case is reported in Fig. 4a. Excitons are promoted by the pump from the ground state GS to E_{22} (second VHS) state, inducing the first photobleaching. The excitons created in E_{22} state relax very fast (in few tens of fs) to the E_{11} state (first VHS). Due to the high pump fluence (10^{14}–10^{15} photons/cm2) and the long E_{11} decay time (few picoseconds [4]), excitons annihilate and repopulate E_{22}. This process, known as exciton–exciton annihilation (EEA), increases the transmittivity of the probe resulting in a second photobleaching channel.

Due to the dipole selection rules, the optical transition from the ground state to E_{22} state is likely when the pump polarization is parallel to the carbon tube [4]. In our experimental condition, the pump polarization is perpendicular to the tube. However, because of in Sample A the pump photon energy (1.5 eV) is resonant with the GS-E_{22} transition (1.3 ± 0.2 eV), a dense population is in anyway photoinduced in the E_{22} state allowing the EEA process. In Sample B, the energy of the GS-E_{22} transition is less resonant with the pump photon energy, thereby reducing the excited carrier density and preventing the EEA.

In order to verify that the positive second dynamics in Sample A is the result of an EEA process, in Fig. 4b the inverse of the transient reflectivity, $(\Delta R/R)^{-1}$, is plotted as a function of the delay time. The quadratic dependence of the temporal evolution of the exciton population on the population itself implies that [10,23,12]:

$$\left(\frac{\Delta R}{R}\right)^{-1} \propto \Delta t \tag{2}$$

where Δt is the delay time between pump pulse and probe pulses. The linear behavior shown in Fig. 4b confirms the non-linear character of the second dynamics in Sample A transient signal. To rationalize our findings, a rate equation model [12,23] is here proposed to interpret the physical processes drawn in Fig. 4a. The temporal evolution of the excitons on the E_{22} state (N_2) and on the E_{11} (N_1) is then determined by:

$$\begin{aligned}\frac{\partial N_2}{\partial t} &= A\cdot G(t) - B\cdot N_2 + \frac{C}{2}\cdot N_1^2 \\ \frac{\partial N_1}{\partial t} &= B\cdot N_2 - D\cdot N_1 - C\cdot N_1^2\end{aligned} \tag{3}$$

where the Gaussian laser pump $G(t) = \left(\sigma\sqrt{2\pi}\right)^{-1} e^{-\frac{t^2}{2\sigma^2}}$ populates the E_{22} state that becomes depopulated by the -BN_2 term where B^{-1} corresponds to the N_2 decay time ($E_{22} \rightarrow E_{11}$). The $CN_1^2/2$ term represents the population of the E_{22} state due to the annihilation of the excitons on the E_{11} state. As a consequence the E_{11} state is populated by the

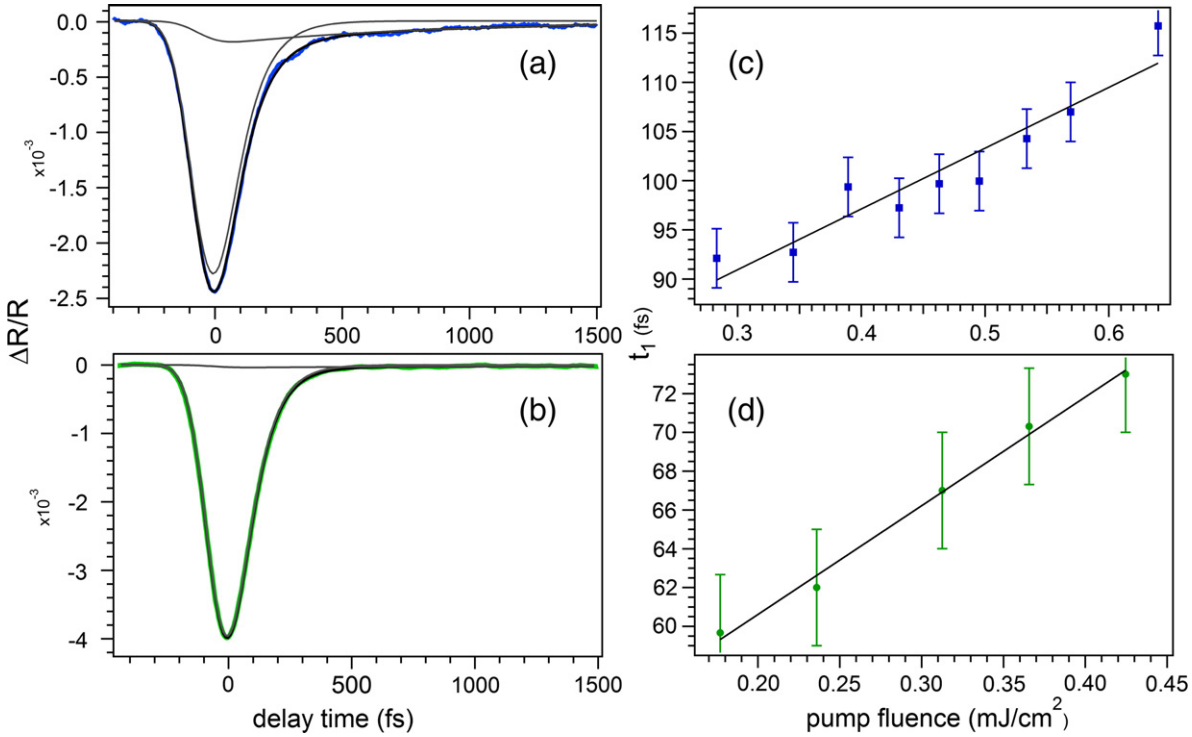

Fig. 3. (a, b) Transient reflectivity signal collected on Sample A and B. The data result well fitted by two and one exponential decay for Sample A and B, respectively. (c,d) Decay time of the first dynamics versus the pump fluence for Sample A and Sample B.

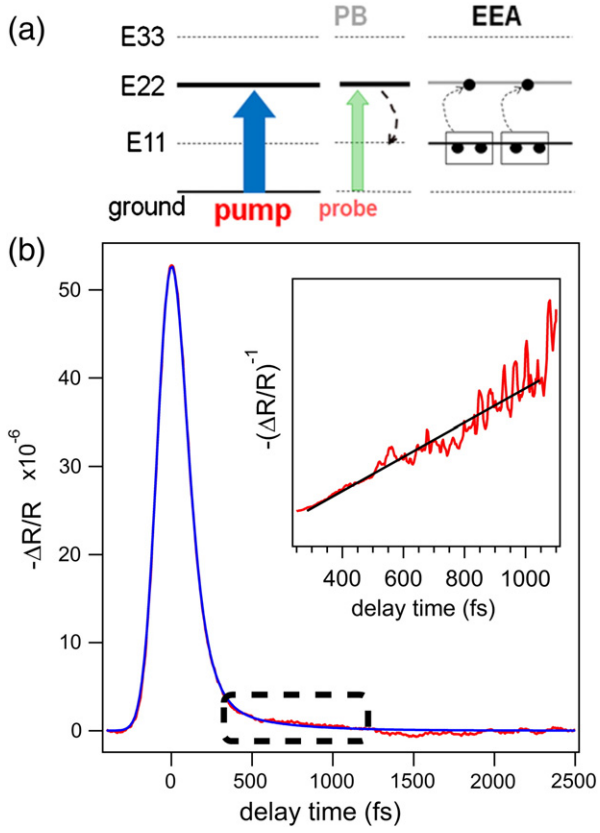

Fig. 4. (a) Sketch of the relaxation processes of the carriers excited in Sample A. (b) Fitting of the transient signal collected on Sample A by using the rate equation model. The linear behavior of the inverse of the transient reflectivity versus the delay time confirms that the second dynamics is ascribed to the exciton–exciton annihilation process.

relaxation of the excitons from the E_{22} state (BN_2) and depopulated by the relaxation into the ground state ($-DN_1$) and by the annihilation process ($-CN_1^2$). The ΔR/R signal is proportional to the N_2 population, the probe photon energy being resonant with the E_{22} state.

As shown in Fig. 4b, the transient response is well approximated by the proposed model. The mean fitted B^{-1} value, for the low fluence spectra, is 65 ± 15 fs. This value is consistent with the value (40 fs) reported for the $E_{22} \rightarrow E_{11}$ decay in SWCNT and with the result previously obtained by interpolating the data with two exponential curves. The fitted D^{-1} value is consistent with the relaxation time of the E_{11} state.

4. Conclusion

In conclusion, by performing transient reflectivity measurements on SWCNT bundles we have shown that the free-electron behavior already observed in unaligned bundles is mainly due to the unalignment. The presence of bundles and a different content of structural defects in the vertically aligned SWCNT reveal an excitonic behavior comparable with that observed in literature on isolated tubes. In order to address the second dynamic revealed in the transient response, a rate equation model involving the exciton–exciton annihilation process has been proposed.

References

[1] P. Avouris, J. Chen, Mater. Today 9 (2006) 46.
[2] P.V. Kamat, J. Phys. Chem. C 111 (2007) 2834.
[3] L. Luer, J. Crochet, T. Hertel, G. Cerullo, G. Lanzani, ACS Nano 4 (2010) 4265.
[4] M. Zheng, E.D. Semke, J. Am. Chem. Soc. 129 (2007) 6084.
[5] S. Reich, C. Thomsen, J. Maultzsch, Carbon Nanotubes. Basic Concepts and Physical Properties, Wiley, 2004.
[6] M.S. Dresselhaus, G. Dresselhaus, Ph. Avouris, Carbon Nanotubes. Synthesis, Structure, Properties, and Applications, Springer, 2001.
[7] D. Eder, Chem. Rev. 110 (2010) 1348.
[8] G. Galimberti, S. Pagliara, S. Ponzoni, S. Dal Conte, F. Cilento, G. Ferrini, S. Hofmann, M. Arshad, C. Cepek, F. Parmigiani, Carbon 49 (2011) 5246.

[9] Sh. Wang, M. Khazov, X. Tu, m. Zheng, D.K. Todd, Nano Lett. 10 (2010) 2381.
[10] Y.-Z. Ma, L. Valkunas, S. Dexheimer, S. Bachilo, G. Fleming, Phys. Rev. Lett. 94 (2005) 157402.
[11] G. Ostojic, S. Zaric, J. Kono, V. Moore, R. Hauge, R. Smalley, Phys. Rev. Lett. 94 (2005) 097401.
[12] Y.-Z. Ma, J. Stenger, J. Zimmermann, S.M. Bachilo, R.E. Smalley, R.B. Weisman, G.R. Fleming, J. Chem. Phys. 120 (2004) 3368.
[13] O. Korovyanko, C.-X. Sheng, Z. Vardeny, A. Dalton, R. Baughman, Phys. Rev. Lett. 92 (2004) 017403.
[14] K. Kato, K. Ishioka, M. Kitajima, J. Tang, R. Saito, H. Petek, Nano Lett. 8 (2008) 3102.
[15] M.S. Dresselhaus, G. Dresselhaus, R. Saito, A. Jorio, Phys. Rep. 409 (2005) 47.
[16] E.F. Antunes, A.O. Lobo, E.J. Corat, V.J. Trava-Airoldi, A.A. Martin, C. Verıssimo, Carbon 44 (2006) 2202.
[17] A.C. Ferrari, J. Robertson, Phil. Trans. R. Soc. A 362 (2004) 2477.
[18] j. Robertson, Mater. Sci. Eng. 37 (2002) 129.
[19] H. Kataura, Y. Kumazawa, Y. Maniwa, I. Umezu, S. Suzuki, Y. Ohtsuka, Y. Achiba, Synth. Met. 103 (1999) 2555.
[20] J.S. Lauret, C. Voisin, G. Cassabois, C. Delalande, Ph. Roussignol, O. Jost, L. Capes, Phys. Rev. Lett. 90 (2003) 057404.
[21] C. Manzoni, A. Gambetta, E. Menna, M. Meneghetti, G. Lanzani, G. Cerullo, Phys. Rev. Lett. 94 (2005) 207401.
[22] G.N. Ostojic, S. Zaric, J. Kono, M.S. Strano, V.C. Moore, R.H. Hauge, R.E. Smalley, Phys. Rev. Lett. 92 (2004) 117402.
[23] Y. Murakami, J. Kono, Phys. Rev. B 80 (2009) 035432.